

AD-A251 049

IDENTIFICATION PAGE

Form Approved
GSA No. 3704-0188

2

Intended to provide a means for the collection, management, and dissemination of information. This document is not to be used for the collection, management, and dissemination of information. This document is not to be used for the collection, management, and dissemination of information. This document is not to be used for the collection, management, and dissemination of information.

"Original contains color
plates. All DTIC reproductions
will be in black and
white"

REPORT DATE
April 303. REPORT TYPE AND DATES COVERED
Interim-91 APR 1 - 92 MAR 31

Annual

5. FUNDING NUMBERS

NEURO-TRIGGERED TRAINING

F49620-90-C-0026

61102F

2313

BS

6. AUTHOR(S)

Alan S. Gevins, PI

Brian A. Cutillo, Co-PI

DTIC
ELECTE

JUN 1 1992

7. PERFORMING ORGANIZATION NAME(S) AND ADDRESS(ES)

EEG Systems Laboratory
51 Federal Street, Suite 401
San Francisco, CA 941078. PERFORMING ORGANIZATION
REPORT NUMBER

9. SPONSORING/MONITORING AGENCY NAME(S) AND ADDRESS(ES)

USAF, AFSC/NL
Air Force Office of Scientific Research
Bldg. 410
Bolling AFB, DC 20332-6448
Dr. Tananay10. SPONSORING/MONITORING
AGENCY REPORT NUMBER

AFOSR-TR- 02 0451

11. SUPPLEMENTARY NOTES

12a. DISTRIBUTION/AVAILABILITY STATEMENT

AFOSR Approved for public release;
distribution unlimited.

12b. DISTRIBUTION CODE

13. ABSTRACT (Maximum 200 words)

In the past year we have made good progress in several areas: 1) most of the major software components for the Neuro-Triggered Training (TRIGGER) system have been implemented; 2) the manuscript of a detailed version of the Working Memory study has been completed for submittal to publication (see 1991 Interim Progress report for short version); 3) analysis of data from a study of linguistic and graphic processes has been completed, graphics are being produced, and a paper is being written for submittal for publication; and 4) the basic methodology of measuring inter-area functional associations is being refined using data from the language study.

14. SUBJECT TERMS

BRAIN ACTIVITY, COGNITION, LEARNING

15. NUMBER OF PAGES

16. PRICE CODE

17. SECURITY CLASSIFICATION
OF REPORT

Unclassified

18. SECURITY CLASSIFICATION
OF THIS PAGE

Unclassified

19. SECURITY CLASSIFICATION
OF ABSTRACT

Unclassified

20. LIMITATION OF ABSTRACT

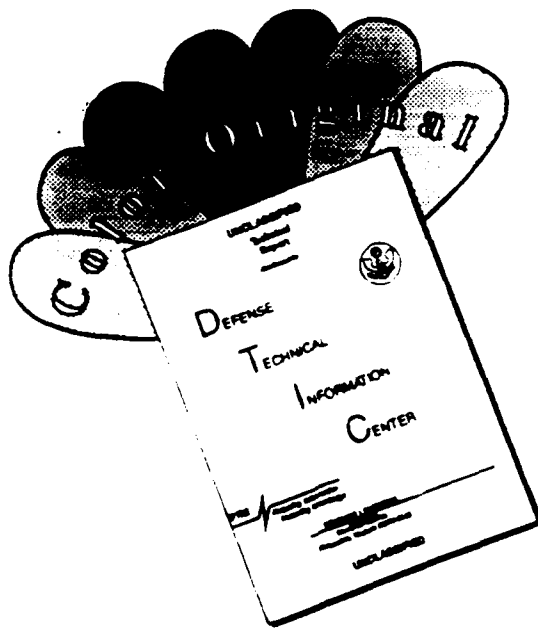
Unlimited

NSN 7540-01-280-5500

Standard Form 298 (Rev. 1-89)
Prescribed by ANSI Z39-18

18 MAY 1992

DISCLAIMER NOTICE



THIS DOCUMENT IS BEST QUALITY AVAILABLE. THE COPY FURNISHED TO DTIC CONTAINED A SIGNIFICANT NUMBER OF COLOR PAGES WHICH DO NOT REPRODUCE LEGIBLY ON BLACK AND WHITE MICROFICHE.

NEURO TRIGGERED TRAINING

AFOSR Contract F49620-90-C-0026

INTERIM TECHNICAL REPORT
1 APR 91 to 31 MAR 92


PREPARED FOR

Dr. John Tangney
Directorate of Life Sciences, AFOSR/NL
Air Force Office of Scientific Research
Bolling AFB, D.C. 20332-6448

APPROVED BY



Alan Gevins, Director



Accession For	
NTIS Grant	<input checked="" type="checkbox"/>
NTIS Task	<input type="checkbox"/>
Unpublished	<input type="checkbox"/>
Justification	
By	
Distribution/	
Availability Codes	
Dist	Avail and/or Special
A-1	

The views and conclusions in this document are those of the authors and should not be interpreted as necessarily representing the official policies or endorsements, either expressed or implied, of the Air Force Office of Scientific Research or the U.S. Government.

92 5 28 050
52 2 22 2 2 2

92-14112


PERSONNEL

Alan Gevins, Principal Investigator
Brian Cutillo, Co-Principal Investigator
James Johnston, Senior Scientist
William O'Connor, Programmer
Michael Ward, Biomedical Engineer

PUBLICATIONS IN THE PAST YEAR

Gevins, A.S., and Cutillo, B.A., (Submitted) Neuroelectric evidence for distributed processing in human working memory.

Gevins, A.S., et al. (In Press, 1992) The future of high-resolution EEGs in assessing neurocognitive effects of mild head injury. In: D. Katz & M. Alexander (Eds), *Journal of Head Trauma Rehabilitation, Special Issue*. Aspen Publishers, Inc.

Gevins, A.S., Le, J., Brickett, P. Reutter, B. and Desmond, J. (1991) Seeing through the skull: Advanced EEGs use MRI's to accurately measure cortical activity from the scalp. *Brain Topography*, 4(2): Human Sciences Press, Inc.: New York, pp. 125-131. [Included]

Gevins, A.S. and Illes, J. (1991) Neurocognitive networks of the human brain. In: Zappulla, R.A. (Ed.) *Windows on the Brain: Neuropsychology's Technological Frontiers*. New York Academy of Sciences: New York, pp. 22-44. [Included]

NEURO-TRIGGERED TRAINING (TRIGGER).

The objective of the Trigger project is to determine the feasibility of a method to accelerate the learning of a task, and optimize its performance by delivering stimuli at instants when preparatory attentional networks are optimal. We plan to achieve this objective by determining the pre-stimulus EEG patterns associated with a subject's accurate task performance using neural-network pattern recognition, and then training the subject to produce those patterns on a single-trial basis.

According to the plan for executing the project, we are currently in the process of checking-out the basic Trigger task presentation and data collection system. Brian Cutillo, the Co-PI, is managing the day-to-day conduct of the project. The programming is being supervised by Jim Johnston, a biophysicist who is experienced in both PC programming and EEG feedback systems. We have adapted existing software to record EEG and behavioral information on a 486 PC, and are redesigning the stimulus presentation and data analysis/display software in a way that will allow easy modification of the Trigger system in the course of future development. For efficiency, a menu system has been written which is used to set and adjust task and feedback parameters during system development and which will be used later when training subjects. The first task implemented has been the Bimanual Visuomotor Task (Gevins et al., 1989a), but the

modular program design will allow the system to utilize other tasks.

Currently the system is able to: 1) present the Bimanual Visuomotor Task with behavioral feedback and end-of-block behavioral summaries, 2) record 9 channels of EEG (right and left hand EMG and EOG will be added later), and the output of 2 finger pressure transducers from a subject performing the task, and 3) online quantify behavioral variables including response time, pressure, duration, accuracy and the adaptive error tolerance. We have set up a small new recording room for this project and cleared it of 60-Hz electromagnetic noise.

Next steps are to:

- 1) Make pilot recordings from several "in house" subjects and use the behavioral variables to form data sets of accurate and inaccurate task trials, statistically balanced for confounding variables (especially response variables).
- 2) Decide what features to use in classifying the accurate and inaccurate trials using the SAM neural network pattern recognition program.
- 3) Program the PC to extract these features on-line.
- 4) Implement an on-line algorithm to detect lateral and vertical eye movements and blinks, and incorrect finger movements or hand EMG activity, and abort the trial if such activity occurs.
- 5) Run the system in full *neurotrigger* mode.

When these goals are achieved, hopefully by the middle of year 3, we will begin pilot recordings to fine tune the system prior to a formal experiment. We may decide to convert the system to the newly developed "in-hat preamp" system. This will require some additional hardware and software modifications, but will result in an more flexible, lower noise system.

REPORT OF RESULTS OF MEMORY STUDY

These are the second set of results obtained from the data recorded from 5 Air Force fighter test pilots several years ago. The first paper was published by the Journal of Electroencephalography and Clinical Neurophysiology (Gevins et al., 1990, Effects of prolonged mental work on functional brain topography, 76:339-350). The second report is titled "Neuroelectric evidence for distributed processing in human working memory", and will be included in our next scheduled report.

STUDY OF LINGUISTIC AND GRAPHIC PROCESSES: AMPLITUDE AND LATENCY ANALYSIS.

Data for this study were previously analyzed and reported in AFOSR Final Technical Report, "Empirical Model of Human Higher Cognitive Brain Function" (March 1990). This material and accompanying graphics are now being prepared for publication, along with some examples of our new method of Finite Element Model Deblurring applied to two of the language subjects for whom we obtained MRI images (see Gevins et al., 1991). We are currently working on the

challenging project of extending our measures of functional association to these cases of 43-channel data.

DEVELOPMENT OF INTERDEPENDENCY MEASURES

Our ongoing development and validation studies of the methods of measuring functional associations between signals from widely distributed areas of the brain is being supervised by Alan Gevins and Brian Cutillo. The other personnel are working under support from grants from NINDS, ONR, and NIMH.

Our current effort is based on detection and separation of evoked-potential (EP) components using a model of linear stochastic mixing. The analysis is currently being carried out on a single-subject recordings of 43-channel Laplacian Derivation language data, and a somatosensory-motor task using a 60-channel chronically-implanted subdural grid. Preliminary results suggest the existence of stable globally coherent spatial patterns corresponding to the EP components. Time-lagged correlations on the EP components that differ across stimulus conditions may yield better measures of interdependency than the untreated timeseries, and may give a better indication of the differential temporal and spatial activation of widely distributed sites of the brain involved in the stages of cognitive processing.

Seeing Through the Skull: Advanced EEGs Use MRIs to Accurately Measure Cortical Activity from the Scalp

Alan Gevins, Jian Le, Paul Brickett, Bryan Reutter, and John Desmond

Summary: There is a vast amount of untapped spatial information in scalp-recorded EEGs. Measuring this information requires use of many electrodes and application of spatial signal enhancing procedures to reduce blur distortion due to transmission through the skull and other tissues. Recordings with 124 electrodes are now routinely made, and spatial signal enhancing techniques have been developed. The most advanced of these techniques uses information from a subject's MRI to correct blur distortion, in effect providing a measure of the actual cortical potential distribution. Examples of these procedures are presented, including a validation from subdural recordings in an epileptic patient. Examples of equivalent dipole modeling of the somatosensory evoked potential are also presented in which two adjacent fingers are clearly separated. These results demonstrate that EEGs can provide images of superficial cortical electrical activity with spatial detail approaching that of O15 PET scans. Additionally, equivalent dipole modeling with EEGs appears to have the same degree of spatial resolution as that reported for MEGs. Considering that EEG technology costs ten to fifty times less than other brain imaging modalities, that it is completely harmless, and that recordings can be made in naturalistic settings for extended periods of time, a greater investment in advancing EEG technology seems very desirable.

Key words: High-resolution EEG; Evoked potential; MRI; Spatial signal enhancement; Deblurring; Finite element model; Laplacian derivation.

Introduction

Although the EEG has been measured for over 60 years, and the averaged evoked potential for over 30, their full potential as brain imaging technologies has not yet been realized. This is not due to an inherent lack of information in EEGs, but to a relative lack of commitment of resources to get at it. The quantity and quality of information obtainable from EEGs is currently limited by the number of scalp recording sites and the amount and type of numerical computing applied. Since the former is only a matter of habit, and since computing has become so powerful and inexpensive, we feel that it is now timely for the imaging capability of EEGs to make a major

advance.

Much of the groundwork for this development has already been accomplished, including recording from more than 100 sites for improved spatial sampling (Gevins et al. 1990), precise measurement and registration of electrode positions with 3-D MRI images (Gevins 1989), means for reducing the spatial blur distortion which occurs when potentials are conducted through the skull (Gevins 1989; Gevins et al. 1990; Le and Gevins In Prep. a,b), computation of the "center of mass" of cortical areas activated by sensory stimulation (equivalent dipoles; Fender 1987), extraction of spatial multivariate features and classification of spatial brain states using neural-network pattern recognition techniques (Gevins 1980; Gevins and Morgan 1988), split-second measures of functional cortical networks (Gevins et al. 1981, 1989), development of quantitative norms for clinical studies (John 1977), and a myriad of other technical developments (reviews in Lopes da Silva et al. 1986; Duffy 1986; Gevins and Remond 1987; Basar 1988; Pfurtscheller and Lopes da Silva 1988; also see special issues of *Brain Topography*, 1989, Vol. 2(1/2), and 1990 Vol 3(1)). Although a considerable effort has already been made in many of these areas, an additional major effort will be required to further refine, integrate and validate EEG spatial enhancement methods, and then to disseminate technologies embodying them.

In considering whether it is worth further developing and modernizing the EEG, it is relevant to note that every

EEG Systems Laboratory and Sam Technology, San Francisco CA, USA.

Accepted for publication: September 23, 1991.

Supported by the National Institute of Neurological Diseases and Stroke, the National Institute of Mental Health, the National Institute of Health, the Air Force Office of Scientific Research, the Air Force School of Aerospace Medicine and the Office of Naval Research. Access to neurosurgery patients was kindly provided by the Northern California Comprehensive Epilepsy Center at the University of California (San Francisco), Dr. Kenneth Laxer, Director, and Dr. Nicolas Barbaro, Neurosurgeon. Contributions to the research presented here were also made by our colleagues at EEG Systems Laboratory including Jim Alexander, Brian Cutillo, Judy McLaughlin, and Michael Ward.

Correspondence and reprint requests should be addressed to Alan Gevins, EEG Systems Laboratory, 51 Federal, San Francisco, CA, 94017, USA.

Copyright © 1991, Human Sciences Press, Inc.

brain imaging modality has its relative strengths and limitations in terms of spatial and temporal resolution, the nature of the processes measured, and economic and logistical factors. For example, while O15 PET is one of the imaging methods with the best spatial resolution, which is approximately 6 to 100 mm for modern PET machines (full width at half maximum; M. Raichle, personal communication; Mintun et al. 1989), O15 PET also has a number of disadvantages which are not often considered: 1) the required time sample of 45-60 seconds is far too long to measure split-second neural processes of seizure generation or of cognition; 2) the experimental designs for PET are highly restricted by safety limitations on allowable dosages of ionizing radiation; and 3) it costs roughly five million dollars for a PET facility. While not comparable to PET in 3-D resolution of many simultaneously active areas throughout the neuroaxis, we believe that improved EEG measures can provide images of superficial cortical activity with a spatial resolution of 1-2 square centimeters, and an unsurpassed millisecond-range temporal resolution. Low cost (in the one hundred to two hundred thousand dollar range), complete harmlessness, ability to record for extended periods of time in a comfortable setting, and opportunity to record the same subject many times make EEG measures additionally attractive.

124-Channel EEG Recordings

Until recently it was assumed by most researchers that, due to the smearing effects of volume conduction, the 19 electrodes of the basic 10-20 system were sufficient for sampling the spatial information of EEG or EP signals at the scalp. This is clearly not the case, as has been amply demonstrated (Lehmann 1986; Wang et al. 1989; Gevins 1989, 1990). Figure 1 is an example which shows that the EEG as normally recorded is spatially undersampled. Isopotential maps are drawn on a scalp surface reconstructed from horizontal MR images of that subject. Data shown are somatosensory evoked potentials to 15-Hz stimulation of the left middle and right index fingers, for a maximum of 122 channels and desampled to 57, 31 and 18 channels. The spline interpolation algorithm makes all the maps visually appealing, but only in the 122-channel version is the presence of two separate peaks obvious, corresponding to the two fingers stimulated.

With the original nineteen electrodes of the 10-20 System (Jasper 1958), the typical distance between electrodes on an average adult male head is about 6 cm; with 124 electrodes, the typical distance is 2.25 cm. This is a good improvement in sampling resolution, but further improvements are possible since the 3 dB point of the point spread function for conductance of potentials from the

brain surface to the scalp averages about 2.5 cm (Gevins 1990). Thus, additional information could be obtained by recording with more electrodes spaced closer together, and then applying signal enhancing methods such as those described below to extract more independent information from each electrode. A good goal for future development is 256 channels which provides an inter-electrode distance of about 1.6 cm.

Previous papers have described our traditional methods for recording EEGs from 124 scalp sites and measuring the three-dimensional position of each electrode (Gevins 1989; Gevins et al. 1990). Advanced systems for very rapid electrode placement and position measurement are currently being refined and tested in our laboratory. The two previous papers have also described our fifth generation EEG analysis software system which is a UNIX-based, network-distributed system written in the C language. A sixth generation system is currently under development in the C++ language. It is also a network-distributed system under UNIX, but it is based on the X-11 network windowing standard and incorporates an object-oriented database technology which will facilitate processing, viewing and retrieving multichannel time series and three-dimensional image data.

MRI Analysis and Modeling Methods

Our approach to 3-D anatomical modeling and visualization has been guided by our need to integrate anatomical data obtained from MRIs with functional data obtained from scalp and cortical EEGs. Although there are now several commercial visualization software packages which can generate 3-D perspective pictures from MRIs, we had to develop our own contouring and surface-based reconstruction techniques and associated MR processing and display methods as we are more concerned with 3-D mathematical modeling of the anatomical structures in the data than with visualization per se. By contrast, the commercial packages are concerned primarily with volume rendering (Levoy 1988; Levin et al. 1989) or surface modeling for visualization using discontinuous "ribbons" (Heffernan and Robb 1985; Jack et al. 1990; implemented by the Analyze software package of the Mayo Foundation) or unstructured lists of triangles created by the "marching cubes" algorithm (Lorenson and Cline 1987; implemented in the apE software package of the Ohio Supercomputer Center).

We developed methods and software to do automated threshold-based 2-D contouring of individual MR images, with optional manual editing, followed by the construction of triangular 3-D surface elements between contours in adjacent images. Our MR images have pic-

ture elements (pixels) with dimensions that are roughly 1 mm by 1 mm, and typically the image planes are separated from one another by 3 mm. Renderings of these surface models are created by using standard 3-D computer graphics techniques (Foley et al. 1990). For example, the surface is "illuminated" by a combination of direct light, skylight, and diffuse light, and the amount of light reflected from the surface to an arbitrary viewpoint is calculated. In addition to generating these realistic surface renderings, we are able to display data such as EPs or event-related covariances (a measure of functional networks — Gevins and Bressler 1988) on these surfaces. This results in powerful images that help to convey the 3-D complexity of anatomical structure and function. Previous papers have described our EEG-MRI alignment procedures (figure 2), as well as our basic MRI image analysis, recognition and visualization methods (Gevins et al. 1990; Reutter and Gevins In Prep.).

EEG Spatial Enhancement Methods

Electrical currents generated by sources in the brain are volume conducted through brain, CSF, skull and scalp to the recording electrodes. Because of this, potentials due to a localized source are spread over a considerable area of scalp and the potential measured at a scalp site represents the summation of signals from many sources over much of the brain. We have developed two spatial enhancement methods to correct this blur distortion; neither method requires specification of an arbitrary source model (e.g., current dipoles).

The simpler method computes a very accurate estimate of the surface Laplacian Derivation (LD), which is proportional to local normal current at the scalp. This has the advantage of eliminating the effect of the reference electrode used for recording, and of eliminating much of the common activity due to either the reference electrode or volume conduction from distant sources. The disadvantages are that the LD does not produce valid values at the outermost ring of electrodes and it does not correct for local differences in skull thickness and conduction properties. Although computing the LD at first seems trivial (Hjorth 1975), there are in fact a number of subtleties (Nunez 1989). The most accurate surface LD, which we have implemented, uses the actual measured electrode positions, and estimates the LD over the actual shape of the head using a 3-D spline algorithm (Le and Gevins In Prep. a). Figure 3 shows the LD for the same data as in figure 1 (lower right). A dramatic increase in spatial detail is apparent with the LD as compared with the linked-ear-reference.

A further improvement in distortion reduction is possible, in principle, by using a finite element model of the cortex, CSF, skull and scalp to estimate the potentials

which would actually be recorded on the surface of the brain. We call our implementation of this method Finite Element Model Deblurring (FEMDB) (Gevins et al. 1990; Le and Gevins In Prep. b). The price of the improvement offered by FEMDB is that MRIs have to be recorded and processed and many more calculations have to be performed. Unlike other methods which estimate cortical potentials or currents (Nicholas and Deloche 1975; Freeman 1980; Hill et al. 1988; Sidman et al. 1989), FEMDB is a true "downward continuation" method in that, without prior knowledge or assumptions about the generating sources, the cortical potential distribution is derived given the scalp potential distribution and a realistic model of the conducting volume between the scalp and cortical surfaces. In the FEMDB, a transformation matrix is constructed based on the geometry and conductivities of the finite elements which predicts the scalp potentials for any given set of cortical potentials. Then an efficient iterative process is used to find the cortical potentials which result in the closest fit between this forward solution and the recorded data. Simulations of the method in a three sphere model showed that the estimated deblurring results are the same as an analytical computation of the exact solution (Le and Gevins In Prep. b). Experiments in which the skull conductivity constant was varied over a 50% range showed smooth and well-behaved effects on FEMDB (Le and Gevins In Prep. b).

Comparison of FEM Deblurring With Subdural Grid Recording

Initial results of FEMDB (figure 4) demonstrate an improvement in detail over the Laplacian Derivation (figure 5) and good agreement between the computed and the actual cortical evoked potentials (figure 6) (Le and Gevins In Prep. b). The data are from a patient with pharmacologically-intractable seizures for whom we have both scalp and subdural grid recordings of the steady-state somatosensory EP elicited by 15-Hz electrical stimulation of the right hand.

Examples of FEM Deblurring

An example is shown of deblurring for a normal male subject who was stimulated with 15 Hz auditory, visual and somatosensory stimuli. Figure 7 shows the deblurred steady-state evoked potentials for stimulation of each of three fingers. Responses to the left and right fingers are appropriately lateralized, and there is an obvious difference between the middle and index finger of the right hand. Figure 8 shows the 15 Hz auditory evoked potential, as well as the visual response to stimulation of the lower left and right visual quadrants.



Figure 1. Steady-state somatosensory evoked potentials elicited by 15-Hz stimulation of left middle and right index finger are shown for an increasing number of channels from 18 to 122. The potential distributions are shown mapped on a reconstructed scalp surface made from that subject's MR images. Only the version with 122 channels shows the true topography, and allows clear visual identification of both the left and right-sided peaks.

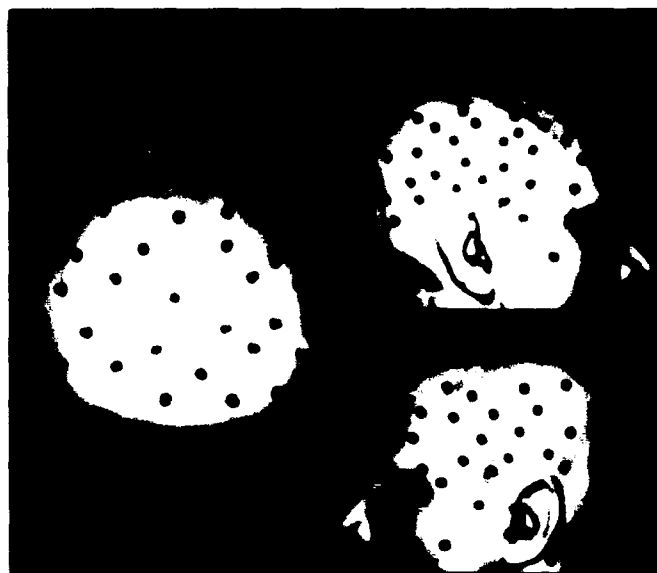


Figure 2. Electrodes are schematically displayed as small purple cylinders, at the actual measured positions, on a 3-D model of the subject's head constructed from his MR images.



Figure 3. Potentials referenced to digitally linked ears (left — same data as figure 1, lower right) and 3-D spline Laplacian Derivation (right) compared for 122-channel, steady-state somatosensory evoked potentials elicited by stimulation of left middle and right index fingers. The Laplacian Derivation clearly isolates peaks that were merged together in the potentials.

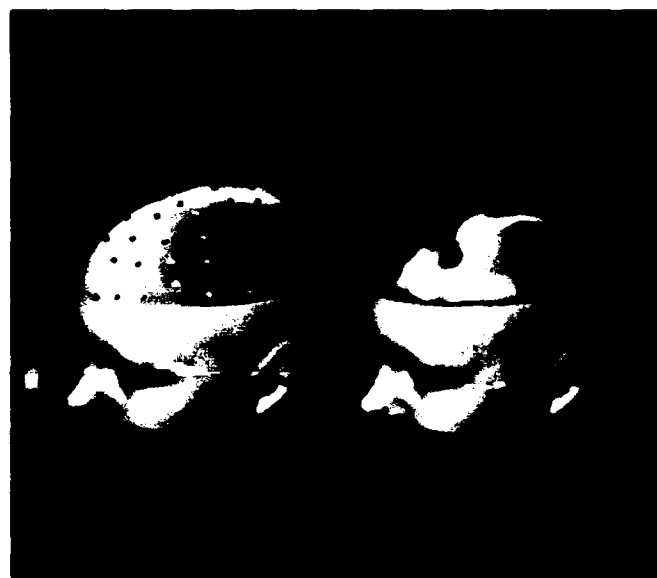


Figure 4. Finite Element Model Deblurring of steady-state somatosensory evoked potentials elicited by 15-Hz stimulation of the left hand of an epileptic patient who had a 64-electrode recording grid implanted for purposes of surgical screening. The single large peak in the potential map (left) is considerably sharpened in the deblurred data (right), which in addition shows some polarity reversals. (All surfaces were reconstructed from horizontal MR images obtained prior to surgery, one of which is shown in part between the scalp and cortex on right.)



Figure 5. Original scalp potentials (left — same data as figure 4, left) and 3-D spline Laplacian Derivation (right). The Laplacian Derivation also is spatially sharpened compared with the original potential data, but is less detailed than the deblurred data shown in figure 4, right.

Deblurred evoked potentials for the visual stimuli show maxima located near the occipital pole, which is the location of the most likely source, striate cortex (area 17). The auditory deblurred evoked potentials are less clearly localized, as would be expected for this more difficult case and the limited accuracy of our initial FEM model, but are more consistent with bilateral temporal-lobe



Figure 6. Comparison of deblurred evoked potentials (left — same data as figure 4, right) with the evoked potentials actually recorded from the subdural grid (right) is shown. The area covered by the grid shows a single large peak similar to that in the deblurred data.

sources than the raw scalp potentials would indicate.

Equivalent-Dipole Source Localization For Somatic and Visual Stimuli

Single equivalent dipole modeling of the head was performed for each of the three 15 Hz somatosensory

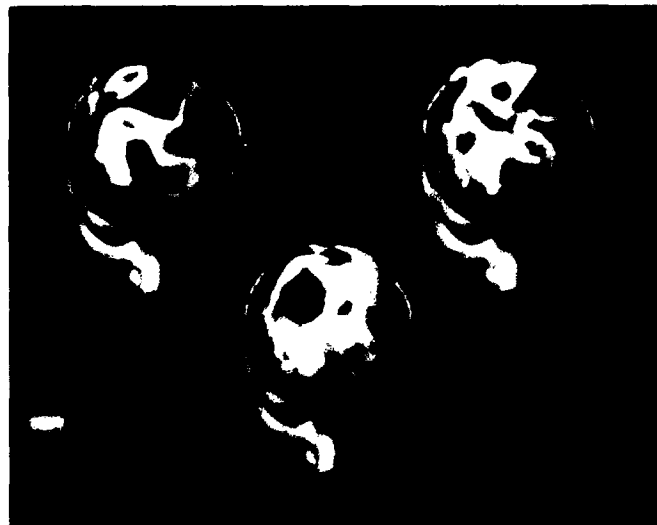


Figure 7. Deblurred steady-state evoked potentials elicited by 15-Hz stimulation of left middle and right middle and index fingers of a normal subject (ms3). All three cases show the expected contralateral maximum in activity, while the response to right index finger stimulation differs markedly from that for the right middle finger.



Figure 8. Deblurred steady-state evoked potentials elicited by 15-Hz auditory and visual stimulation. Rear view of the head shows maximal activity at the occipital pole for the parafoveal right and left visual quadrant stimulation. The auditory response is less clear, but is greater over the right hemisphere.



Figure 9. Single equivalent dipole modeling for each of the three 15-Hz somatosensory stimulus conditions shown in figure 7. Dipoles are shown with respect to the scalp surface and a cubic brain model constructed from the subject's MR images. Each dipole is represented as a disk with its center on the dipole's location, and with a cone pointing in the dipole's direction. Dipole color indicates stimulus as follows: left middle finger (blue), right middle (red), and right forefinger (yellow). Each dipole appears in the contralateral hemisphere, and the dipole for the forefinger is located slightly more lateral than that for the middle finger, consistent with the known locations of the somatosensory projection areas.

stimulus conditions shown in figure 7. Figure 9 shows the dipoles with respect to the scalp surface and a cubic brain model constructed from the subject's MRI (see Gevins et al. 1990). Each dipole is represented as a disk with its center on the dipole's location, and with a cone pointing in the dipole's direction. Dipole color indicates stimulus as follows: left middle finger (blue), right middle (red), and right forefinger (yellow). The goodness of fit was 85, 96 and 97% for right forefinger, right middle finger, and left middle finger, respectively. Each dipole appears in the contralateral hemisphere, and the dipole for the forefinger is located slightly more lateral than that for the middle finger, consistent with the known locations of the sensory projection areas and other physiological source localization results (Okada et al. 1984; Wood et al. 1985; Luders et al. 1986). Although dipole models are not physiologically realistic, they are nonetheless useful for locating the center of mass of primary sensory cortex. Although some proponents of MEG technology have maintained otherwise, equivalent dipole modeling performed with EEG appears to be no less accurate than that performed with MEG. This same

conclusion has recently been demonstrated via direct comparison of MEG and EEG localization for dipoles generated by stimulation of electrodes implanted in epileptic patients (Cohen et al. 1990).

Conclusion

Although hundreds of millions of dollars have been invested in developing other forms of functional brain imaging including PET, SPECT, MRSI, and MEG, the EEG has been relatively overlooked by the scientific, medical and business community at large. This is unfortunate since it is clear that EEGs, coupled with MRIs, are capable of providing images of superficial cortical electrical activity with very high temporal resolution and spatial detail approaching that of O15 PET scans. EEGs are inherently a low cost technology. They require neither bulky, expensive sensor technologies, nor ionizing radiation. We sincerely hope that EEG will receive the attention and subsequent large-scale development that it merits.

References

- Basar, E. (Ed.). *Dynamics of Sensory and Cognitive Processing by the Brain*. Springer-Verlag, Heidelberg, 1989.
- Cohen, D., Cuffin, B.N., Yunokuchi, K., Maniewski, R., Purcell, C., Cosgrove, G.R., Ives, J., Kennedy, J.G. and Schomer, D.L. MEG versus EEG localization test using implanted sources in the human brain. *Ann. Neurol.*, 1990, 28: 811-817.
- Duffy F.M. (Ed.). *Topographic Mapping of Brain Electrical Activity*. Butterworths, Boston, 1986.
- Fender, D.H. Source localization of brain electrical activity. In: A.S. Gevins and A. Remond (Eds.), *Handbook of Electroencephalography and Clinical Neurophysiology: Vol. 1, Methods of Analysis of Brain Electrical and Magnetic Signals*. Elsevier, Amsterdam, 1987: 355-403.
- Foley, J.D., van Dam, A., Feiner, S.K. and Hughes, J.F. *Computer Graphics: Principles and Practice*, 2nd Ed. Addison-Wesley, New York, 1990.
- Freeman, W.J. Use of spatial deconvolution to compensate for distortion of EEG by volume conduction. *IEEE Trans. Biomed. Engr.*, 1980, 27: 421-429.
- Gevins, A.S. Application of pattern recognition to brain electrical potentials. *IEEE Trans. Pattern Ana. Mach. Intell.*, 1980, 12: 38.
- Gevins, A. Dynamic functional topography of cognitive tasks. *Brain Topography*, 1989, 2: 37-56.
- Gevins, A.S. Dynamic patterns in multiple lead data. In: J.W. Rohrbaugh, R. Parasuraman and R. Johnson, Jr. (Eds.), *Event-Related Brain Potentials: Basic Issues and Applications*. Oxford University Press, New York, 1990: 44-56.
- Gevins, A.S. and Bressler, S.L. Functional topography of the human brain. In: G. Pfurtscheller and F.H. Lopes da Silva (Eds.), *Functional Brain Imaging*. Hans Huber Publishers, Bern, 1988: 99-116.
- Gevins, A.S. and Morgan, N.H. Applications of neural-network

- (NN) signal processing in brain research. *IEEE ASSP Trans.*, 1988, 7: 1152-1161.
- Gevins, A.S. and Remond, A. (Eds.). *Methods of Analysis of Brain Electrical and Magnetic Signals. Handbook of Electroencephalography and Clinical Neurophysiology*, Vol.1. Elsevier, Amsterdam, 1987.
- Gevins, A.S., Bressler, S.L., Morgan, N.H., Cuttillo, B.A., White, R.M., Greer, D.S. and Illes, J. Event-related covariances during a bimanual visuomotor task. I. Methods and analysis of stimulus- and response-locked data. *Electroenceph. Clin. Neurophysiol.*, 1989, 74: 58-75.
- Gevins, A.S., Doyle, J.C., Cuttillo, B.A., Schaffer, R.E., Tannehill, R.S., Ghannam, J.H., Gilcrease, V.A. and Yeager, C.L. Electrical potentials in human brain during cognition: New method reveals dynamic patterns of correlation. *Science*, 1981, 213: 918-922.
- Gevins, A., Brickett, P., Costales, B., Le, J., Reutter, B. Beyond topographic mapping: Towards functional-anatomical imaging with 124-channel EEGs and 3-D MRIs. *Brain Topography*, 1990, 3: 53-64.
- Heffernan, P.B. and Robb, R.A. A new method for shaded surface display of biological and medical images. *IEEE Trans. Medical Imaging*, 1985, 4: 26-38.
- Hill, C.D., Kearfott, R.B. and Sidman, R.D. The inverse problem of electroencephalography using an imaging technique for simulating cortical surface data. In: R. Vichnevetsky, P. Borne, J. Vignes (Eds.), *Proc. 12th IMACS World Cong.*, Vol. 3, 1988: 735-738.
- Hjorth, B. An on-line transformation of EEG scalp potentials into orthogonal source derivations *Electroenceph. Clin. Neurophysiol.*, 1975, 39: 526-530.
- Jack, C.R., Marsh, W.R., Hirschorn, K.A., Sharbrough, F.W., Cascino, G.D., Karwoski, R.A. and Robb, R.A. EEG scalp electrode projection onto three-dimensional surface rendered images of the brain. *Radiology*, 1990, 176: 413-418.
- Jasper, H.H. The ten-twenty electrode system of the international federation. *Electroenceph. Clin. Neurophysiol.*, 1958, 10: 371-375.
- John, E.R. *Neurometrics: Clinical Applications of Quantitative Electrophysiology*. Lawrence Erlbaum, Hillsdale, NJ, 1977.
- Le, J. and Gevins, A.S. Laplacian derivation of scalp-recorded EEGs computed with realistic head model and 3-D spline. In preparation, a.
- Le, J. and Gevins, A.S. MRI-based finite element model deblurring of scalp-recorded EEGs. In preparation, b.
- Lehmann, D. Spatial analysis of EEG and evoked potential data. In: F.H. Duffy (Ed.), *Topographic Mapping of Brain Electrical Activity*. Butterworths, Boston, 1986: 23-61.
- Levin, D.N., Hu, X., Tan, K.K. and Galhotra, S. Surface of the brain: three-dimensional MR images created with volume-rendering. *Radiology*, 1989, 171: 277-280.
- Levoy, M. Display of surfaces from volume data. *IEEE Comput. Graph. and Applic.*, 1988, 8: 29-37.
- Lopes da Silva, F.H., Storm van Leeuwen W. and Remond, A. (Eds.). *Handbook of Electroencephalography and Clinical Neurophysiology*, Vol. 2: Clinical Applications of Computer Analysis of EEG and other Neurophysiological Signals. Elsevier, Amsterdam, 1986.
- Lorensen, W. E. and Cline, H. E. Marching cubes: A high resolution 3-D surface construction algorithm. *Comput. Graph.*, 1987, 21: 163-170.
- Luders, H., Dinner, D.S., Lesser, R.P. and Morris, H.H. Evoked potentials in cortical localization. *J. Clin. Neurophysiol.*, 1986, 3: 75-84.
- Mintun, M.A., Fox, P.T. and Raichle, M. A highly accurate method of localizing regions of neuronal activation in the human brain with positron emission tomography. *J. Cereb. Blood Flow Metab.* 1989, 9: 96-103.
- Nicholas, P. and Deloche, G. Convolution computer processing of the brain electrical image transmission. *Int. J. Bio-Med. Comput.*, 1976, 7: 143-159.
- Nunez, P. Estimation of large scale neocortical source activity with EEG surface Laplacians. *Brain Topography*, 1989, 2: 141-154.
- Okada, Y.C., Tannenbaum, R., Williamson, S.J. and Kaufman, L. Somatopic organization of the human somatosensory cortex revealed by neuromagnetic measurement. *Exp. Brain Res.* 1984, 56: 197-205.
- Pfurtscheller, G. and Lopes da Silva, F.H. (Eds.). *Functional Brain Imaging*. Hans Huber Publishers, Bern, 1988.
- Reutter, B.W. and Gevins, A.S. Algorithms for analysis of Magnetic Resonance Images. In preparation.
- Sidman, R.D., Kearfort, R.B., Major, D.J., Hill, D.C., Ford, M.R., Smith, D.B., Lee, L. and Kramer, R. Development and application of mathematical techniques for the noninvasive localization of the sources of scalp-recorded electric potentials. In: J. Eisenfield and D.S. Levine (Eds.), *IMACS Trans. Scientific Computing*, Vol. 5. J. C. Baltzer AG, Basel, 1989: 133-157.
- Wang, J., Cohen, L.M. and Hallett, M. Scalp topography of somatosensory evoked potentials following electrical stimulation of femoral nerve. *Electroenceph. Clin. Neurophysiol.*, 1989, 74: 112-123.
- Wood, C.C., Cohen, D., Cuffin, B.N., Yarita, M. and Allison, T. Electrical sources in human somatosensory cortex: Identification by combined magnetic and potential recordings. *Science*, 1985, 227: 1051-1053.

Reprinted from *Windows on the Brain*
Volume 620 of the *Annals of the New York Academy of Sciences*
April 24, 1991

Neurocognitive Networks of the Human Brain^a

ALAN S. GEVINS AND JUDY ILLES

*EEG Systems Laboratory
51 Federal Street
San Francisco, California 94107*

INTRODUCTION

Among the techniques for studying brain-behavior relationships in humans, scalp-recorded neural potentials have been used widely for over 50 years. With the technological advances of the 1970s and 1980s, new recording and analysis tools have been developed for obtaining increasingly specific information about the spatial and temporal features of neurocognitive processes. Such advances have made possible neuroelectric recordings with many channels, well beyond the original 19 channels of the international 10-20 system proposed by Jasper¹ in the 1950s. These tools have also provided improved signal processing and means of correlating neuroelectric measures with anatomical information from magnetic resonance images. We will focus on these tools in the first part of this chapter; in the second part, we will describe how we have been applying the tools to study the split-second components of higher cognitive functions.

TOOLS OF THE TRADE

Improved Spatial Sampling

Electrode Arrays with 125 Channels

One of the requirements for extracting detailed information about cognitive processes from the scalp-recorded EEG is to have adequate spatial sampling. The 19 channels customarily employed in clinical recordings provide an interelectrode distance of about 6 cm. While this is sufficient for detecting signs of gross pathology, it is obviously insufficient for resolving functional differences within small cortical regions. To improve spatial resolution, we have been making 59-channel recordings for the past

^aSupported by grants from the National Institute of Neurological Diseases, the National Institute of Mental Health, the Air Force Office of Scientific Research, and the National Science Foundation.

several years. This provides an interelectrode distance of about 3.5 cm on a typical adult head, which is still not good enough. To improve sampling, we recently developed a 125-channel recording system that provides an interelectrode distance of about 2.25 cm. Subjects wear a stretchable EEG recording cap, with electrodes placed on the cap according to an expanded version of the standard international 10-20 system.² Prior to each EEG recording session, the 3-D position of each electrode on the individual subject's head is measured precisely with a commercial 3-D digitizer (FIG. 1). To date 12 full-scale 125-channel recordings have been made from subjects receiving visual, auditory, and somatic stimuli.

Registration of Scalp-Electrode Positions with Underlying Anatomical Structures

To visualize the brain areas underlying the scalp electrodes, a procedure is needed for aligning scalp-electrode positions and underlying anatomical structures. This first requires producing an accurate anatomical representation of a subject's brain.

Distortion Correction of Magnetic Resonance Images. While magnetic resonance (MR) images are invaluable because of the anatomical differentiation they provide, they contain inherent distortion that, if not corrected, may cause quantitative measurements of position, length, area, and volume to be erroneous. The distortion can exceed 10% and commonly arises from calibration errors and inhomogeneities of the magnetic field gradients. We have been working on correcting this problem using both phantom calibration data and data recorded from human subjects wearing constructed helmets with spherical fiducial markers that are easily visualized on MR images. It is necessary to correct both image intensity and image position.

To test our methods, scans from a Diasonics MTS MR system were made on three subjects. The maximum total distortion measured on this machine was 8%. Variation between images with TR = 600 msec and TE = 20 msec and images with TR = 2000 msec and TE = 35 and 70 msec were found to be less than 2%. We compared the location of the spherical fiducial markers in coronal, sagittal, and axial images, and various image transforms were then used to bring the measured points into alignment. We found that by computing a separate scale factor for each direction combined with a translation and rotation, two sets of images could be brought into reasonably close alignment. An example of a set of Diasonics MRIs before correction is shown in FIGURE 2A. It is clear that the anatomical positions corresponding to the scalp and cranium do not line up. The coronal sections shown in blue are shifted to the left of their correct position. The sagittal sections shown in reddish brown are "stretched" by approximately 17% in the anterior/posterior direction compared to the horizontal or transaxial sections which are shown in dark green. The same images after correcting for distortion are shown in FIGURE 2B.

Alignment of EEG Electrode Positions with MR Surface Reconstructions. A linear transformation is calculated to superimpose electrode positions and the scalp-surface contours obtained from MR images. This transformation is initially determined by visually adjusting a graphical display of the electrodes and scalp contours. An optimal transformation is then calculated by a program that adjusts each parameter in the transformation until the average distance between all electrode positions and the closest scalp point is minimized (FIG. 3). The aligned surface model can also be superimposed onto composite MR images showing various orientations (FIG. 4). Additionally, surfaces may be constructed by manually tracing other structures on each MR image and then calculating the polygonal surface which fits these contours (FIG. 5).

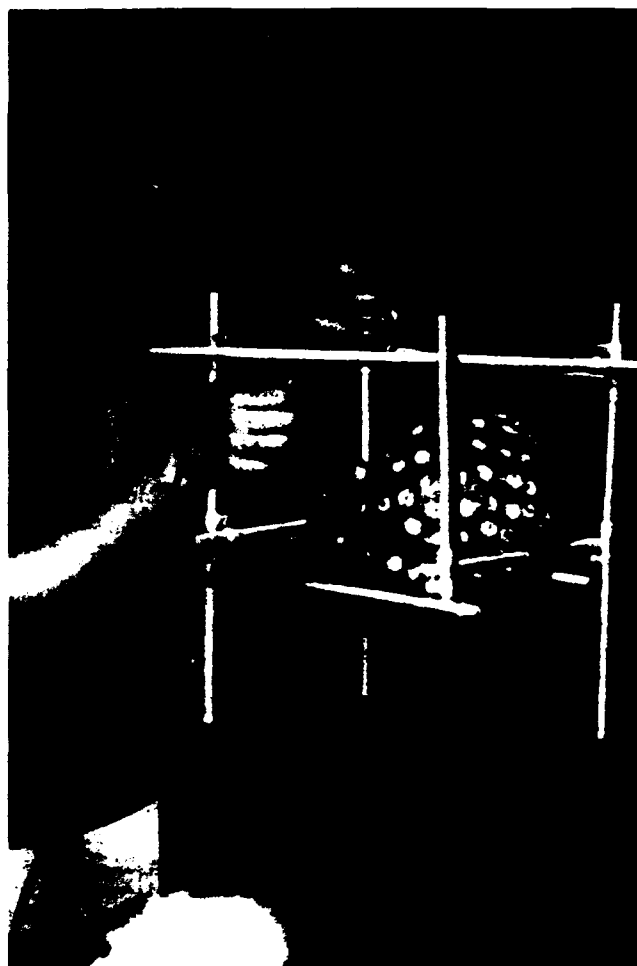


FIGURE 1. Digitization of scalp electrode positions. The subject is resting in a headrest designed to minimize head movement. The technician touches the stylus (which contains electromagnetic field sensors for x, y, and z axes) to each of the electrodes in turn. The 3-D coordinates of each electrode position are transmitted to the data collection and analysis computer.

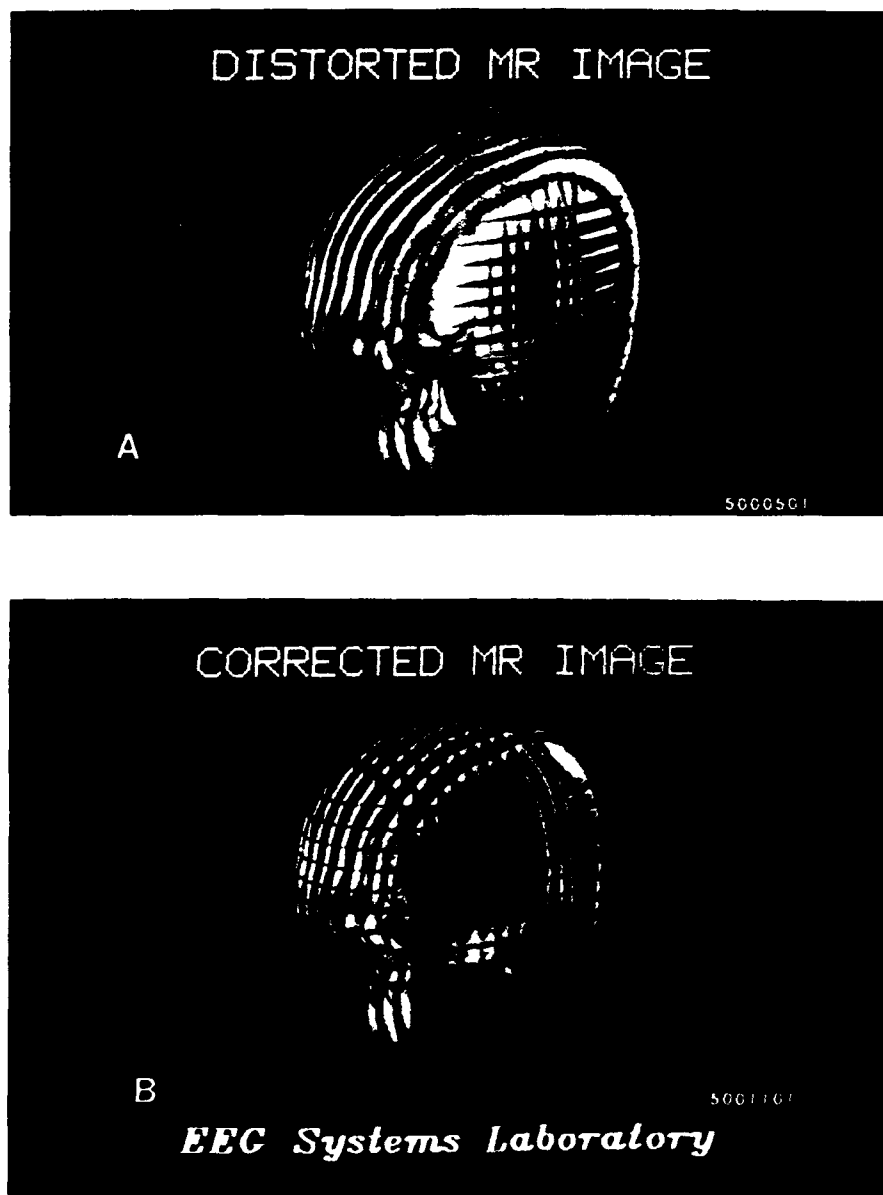


FIGURE 2. (A) Composite of distorted MR images in horizontal, sagittal, and coronal orientations as originally recorded. The location of the scalp is not consistent for different orientations. (B) Composite of the same images after transformation to correct for distortion. The scalp surface now appears at the same location in all orientations.

FIGURE 3. Rough sagittal view of 128-electrode montage constructed from horizontal MR images and positioned on the scalp surface. Also shown is the coordinate system with the origin located halfway between the T3 and T4 temporal electrodes. Some electrodes are not properly aligned with the scalp surface due to a mechanical problem that has been corrected.

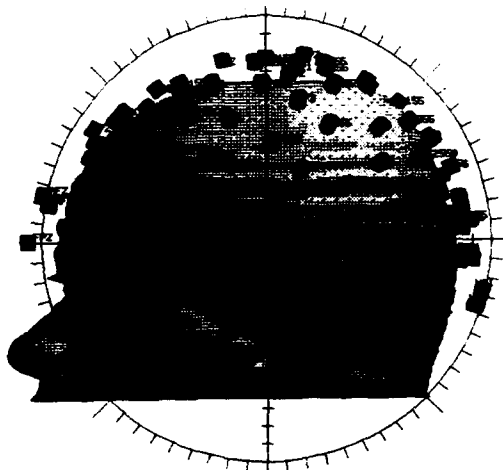


FIGURE 4. Rough surface reconstruction of the scalp from horizontal MR slices with a cutaway to show horizontal, sagittal, and coronal MR images of the left frontal lobe. In this early reconstruction, the sagittal and horizontal slices are not entirely aligned, causing the sagittal section to protrude from the surface.



FIGURE 5. Reconstruction of the right hemisphere of the brain and spinal cord viewed from the (A) right and (B) anteriorly.



Reduction of Brain Potential Blur Distortion

Laplacian Derivation. Neuroelectric signals recorded at the scalp are principally distorted by transmission through the low-conductance skull. This distortion manifests as a spatial low-pass filtering which causes the potential distribution at the scalp to appear blurred or out of focus. There are a number of methods for reducing this distortion, among which the spatial Laplacian operator is perhaps the simplest and most effective. This method, which is often referred to as the Laplacian derivation, is derived by computing the second derivative in space of the potential field at each electrode. This converts the potential into a quantity proportional to the current entering and exiting the scalp at each electrode site, and eliminates the effect of the reference electrode used during recording. An approximation to the Laplacian derivation, introduced by Hjorth^{3,4} assumes that electrodes are equidistant and at right angles to each other. Although this approximation is fairly good for some electrode positions such as midline central (Cz), it is less accurate for others such as midtemporal (T5). We have been using a more accurate estimate of the Laplacian derivation that is based on projecting the measured electrode positions onto a two-dimensional surface. Although this produces a dramatic improvement in topographic detail, some problems remain because of the assumptions that surrounding electrodes used to estimate the Laplacian of an electrode are near that electrode and that the current gradient is uniform over the region encompassed by the surrounding electrodes. Furthermore, it is not possible to estimate the Laplacian at peripheral electrodes because the surrounding electrodes are incomplete.

Spatial Deconvolution Using Spherical Head Model. By modeling the tissues between brain and scalp as surfaces with different thicknesses and resistances, we have performed a deblurring operation that, in principle, makes the potential appear as if it were recorded just above the level of the brain surface,⁵ without assumptions about the actual (cortical or subcortical) source locations. The deblurring operation, however, requires detailed modeling of the tissues which, when the exact shape of the head is taken into account, is a great deal of work. The operation is even further complicated by the fact that a solution to calculating the local resistance of the skull precisely does not yet exist. With the conduction of potentials from a localized source spread over a considerable area of scalp, the summation of signals at any given scalp site may reflect many sources over much of the brain. In the context of a four-shell spherical head model, we have estimated the amount of spread—the “point spread”—for a radial equivalent dipole source in the cortex to be about 2.5 cm. If the conductance of the skull is known, a deblurring operation using a model-based deconvolution can, in principle, achieve a better signal enhancement than a Laplacian derivation when the distance between electrodes is less than approximately the point spread distance of 2.5 cm.

Finite Element Method. Another method of increasing spatial resolution for those cases for which the source generators can be modeled as current dipoles, and for which MR data is available, is the finite element method (FEM). The entire volume of the head, as found in MR images, is broken up into many small elements representing various tissues: the scalp, skull, and brain. By assigning each element a conductivity constant (obtained from textbook values) and one for a known source, it is possible to calculate the potential at each vertex of all the finite elements using Maxwell's equations. Because the number of vertices is approximately 10,000, an efficient algorithm is necessary to make this practical on a small computer. Using a SUN Sparc-1 workstation rated at about 12 MIPS, the initial matrix decomposition based on a set of finite elements takes about 90 min, while the potential computation for each source takes

6 min. If a practical method can be developed for estimating local skull conductance, the FEM deblurring method has the capability of producing highly enhanced representations of the current distribution on the exposed surface of the cortex.

Detecting Artifacts

The usual practice in evoked potential studies of cognition is to reject automatically artifacted trials in which the voltage of the eye-movement measurement channels exceeds a fixed threshold.⁶ While this procedure catches large contaminants, it entirely misses small ones. This can lead to a spurious result if there are small, but consistent saccades or microblinks approximately time-locked to stimulus presentation. Although we also use an on-line artifact detection procedure to flag automatically portions of trials and individual electrodes that have unusually high or low amplitude, all data are examined visually on a graphics terminal to confirm and improve the computer's detections as needed. In our studies with clinically healthy, young adult subjects, there is about 10% data attrition due to artifacts.

Data Set Formation: Controlling for Spurious Sources of Variance

After the data have been cleared of instrumental and subject-related artifacts, data sets are usually formed in pairs to test specific hypotheses. In forming these data sets, it is imperative that the major difference between two sets be related to the hypothesis being tested. It is, of course, standard practice to try to eliminate spurious differences by careful experimental design, but there is always the chance that some remaining factors differ between sets. These uncontrolled factors can include small residual eye-movement contaminants, arousal level, and response movement parameters (e.g., force or reaction time), all of which are known to affect neuroelectric signals.

To ascertain that the major source of variance is actually related to the hypothesis, the two sets of artifact-free trials are submitted, usually on a subject-by-subject basis, to an interactive program that displays the means, *t* tests, and histogram distributions of up to 50 behavioral and physiological event variables. These include stimulus parameters, reaction time, movement magnitude and duration, error, EEG arousal index, eye-movement, muscle potential indices, and so on. The data sets are inspected for significant differences in variables which are not related to the hypothesis, and outliers are discarded. As an example, an unintentional difference between experimental conditions in response force may be present. In the data set with the larger response force, the associated movement-related potentials could overlap the P300 evoked potential peak causing a spurious between-condition difference in P300 amplitude. After careful balancing of the data sets for such movement parameters, valid assessments about P300 peak effects may be made. In balancing our data we are careful not to truncate the histogram distribution severely. The unrelated variables are reduced to a between-condition alpha significance of 0.2, or if this is not possible without seriously affecting the distribution, to just over 0.05. The net effect of these procedures is the certainty that when a neuroelectric difference between experimental conditions is found, the difference actually relates to the hypothesis under consideration.

Neurocognitive Pattern Analysis

We have been using the term "neurocognitive pattern analysis" (NCP analysis) to refer to our procedures for extracting task-related spatiotemporal patterns from the unrelated background activity of the brain. In the first of three generations of NCP analysis, we measured background EEG spectral intensities while people performed complex tasks, such as arithmetic problems lasting up to one minute. These patterns had sufficient specificity to identify the type of task,^{7,8} but when the tasks were controlled for stimulus-, response-, and performance-related factors, they had identical, spatially diffuse EEG spectral scalp distributions.⁷ This study suggested that complex tasks involving a variety of sensory, cognitive, and motoric processes activate large, widespread areas of cortex to a degree proportional to the subject's effort. It also strongly suggested that most studies of EEG correlates of cognitive activities, including those of hemispheric lateralization, may have confounded electrical activity related to limb and eye movements, stimulus properties, and task difficulty with those of mental activity *per se*.

In the second generation of NCP analysis, we measured cross-correlations between electrodes recorded during performance of simple visuomotor judgment tasks.⁹ From this experiment, in which rapidly shifting focal patterns were extracted from two similar spatial tasks, it was clear that a split-second temporal resolution is imperative for isolating the rapidly shifting neurocognitive processes associated with successive information processing stages.

In the third generation, we extended our methods to include event-related covariances (ERCs). The ERC approach is based on the hypothesis that when regions of the brain are functionally related, their event-related potential (ERP, another name for evoked potential) components are related in shape and in time.¹⁰ The idea is that the ERP waveform delineates the time course of event-related mass activity of a neural population, so that if two populations are functionally related, their ERPs should line up in time, perhaps with some delay. If so (and if the relationships are linear as they often appear to be), this could be measured by the lagged covariance between the ERPs, or portions of the ERPs, from different regions (FIG. 6). This is the event-related covariance method.

The procedures that are followed for ERC analysis are described here. Procedures 1-4 have been discussed in detail above.

1. A sufficient amount of data are recorded using as many electrodes as possible.
2. Data with artifact contamination are removed.
3. Pairs of conditions to be compared are selected, and trials with extreme values of behavioral variables are eliminated.
4. The Laplacian operator is applied to the potential distribution of each non-peripheral scalp-electrode location.
5. Analysis intervals and digital filter characteristics are determined. The analysis intervals are usually either centered on an ERP peak, or are positioned just before or after a stimulus or response.
6. Enhanced, filtered, and decimated averaged Laplacian ERPs for each condition are computed. (In an optional procedure, used when the signal-to-noise ratio is very low, a statistical procedure is used to identify trials with measurable event-related signals, and averages are formed only from those trials.¹¹)
7. Multilag cross-covariance functions are computed between all pairwise channel combinations of these averaged ERPs in each selected analysis window. The

magnitude of the maximum value of the cross-covariance function and its lag time are the features used to characterize the ERC. The covariance analysis interval is the width of one period of the band-center frequency of each filter. Down-sampling factors are determined by the 20 dB rejection point, and the covariance function is computed up to a lag time of one-half period of the high frequency for each band. For example, we often use a filter with 3 dB cutoffs at 4 and 7 Hz, and with 20 dB attenuation at 1.5 and 9.5 Hz. The filtered time series are decimated from 128 to 21 Hz for each covariance calculation. Covariance is estimated over a 187-msec window, which corresponds to one period of a 5.5-Hz sinusoid. Each window is lagged by up to 8 lags at the original undecimated sampling rate, i.e., one hundred-twenty-eighth of a second per lag.



FIGURE 6. Schematic diagram showing the relationship of an event-related covariance (ERC) line on a top view of a model head (*left*) to the theta-band-filtered, averaged event-related Laplacian derivation waveforms (*right*). ERCs were computed over the indicated 187-msec analysis interval from the aPz and aCz electrode sites. The width of an ERC line indicates the significance of the covariance between two waveforms, with the scale appearing above the word "significance." The color of the line indicates the time delay in msec (lag time of maximum covariance) as shown in the scale above "msec delay." The color of the arrow indicates the sign of the covariance (same color as line = positive; skin color = negative). The arrow points from leading to lagging channel, unless there is no delay, in which case a bar is shown. The covariance between aPz and aCz is significant at $p < 10^{-5}$. The aPz waveform leads the aCz waveform by about 16-31 msec (*green line*), and the covariance is positive (*green arrow*) (From Gevins *et al.*¹⁷)

8. The significance of ERCs is determined by reference to an estimate of the standard deviation of the "noise" ERC. The noise ERC is computed by averaging random intervals in each single trial of the ensemble of trials. ERC analysis is then performed on a filtered and decimated version of the resulting "noise" averages, yielding a distribution of "noise" ERCs. The threshold for significance is reduced according to the dimensionality of the data with Duncan's correction procedure. The number of channels is used as a conservative estimate of the number of independent dimensions. The most significant ERCs in each interval are graphed.
9. ANOVA and post-hoc *t* tests are used to compare ERC patterns between conditions. The similarity of appearance of two ERC graphs is measured with an estimate of the correlation between them. The estimate comes from a distribution-independent "bootstrap" Monte Carlo procedure,¹² which also yields a confidence interval for the estimates.
10. The between-subject variability of ERC patterns is tested by determining whether each pair of experimental conditions of a particular subject can be distinguished using discriminating equations generated on the other subjects.
11. The within-subject reliability is assessed by attempting to discriminate the experimental conditions for each session using equations generated on that subject's other sessions.

The tests of both between- and within-subject variability and reliability are performed on sets of single trials. This quantifies the extent to which the condition-specific patterns from the ERC analysis of the average ERPs can be observed in each trial. Although this procedure could be done with any type of discriminant analysis, we have developed the use of distribution-independent, layered, artificial "neural network" pattern classification algorithms for this purpose.^{13,14} We have shown that this method has better sensitivity than stepwise or full-model linear or quadratic discriminant analysis.¹⁵ The pattern recognition approach has the advantage of testing how well a subject's individual trials conform to those of the group in discriminating two behavioral conditions of interest. In the same way, the trials of each session of a subject are tested by conformity to trials from the other sessions of that subject. Requiring trial-by-trial discriminability is a strict condition for deciding between-subject variability and within-subject reliability.

Each subject's classification yields a score, which is the percent of trials that are correctly classified by the group discrimination equations. The score is assessed for significance by comparison to the binomial distribution.¹⁵ A significant classification score for a subject indicates that the group equations are successful in discriminating the two conditions in his or her trials.

Within-subject (between-session) reliability is tested in a similar manner. The trial set (consisting of the two conditions) from each of a subject's sessions is tested with equations developed on the trial sets from his or her other sessions. The single-trial ERC values come from channel pairs that are significant in the ERC pattern formed from the average over all his or her sessions. Post-hoc comparisons are valuable in determining whether effects of learning and/or habituation are evident over sessions, by indicating which sessions are alike and where transitions occur between sessions.

FIGURE 7 is a block diagram of the data collection and analysis process discussed above. For studies not requiring pattern recognition analysis, the event-related covariances are computed on averaged event-related potentials after band-pass filtering.

In the next section, results of a study of bimanual visuomotor performance and a study of the effects of mental fatigue on human cognitive networks are presented. Preliminary results of a study of elementary language processes are also described.

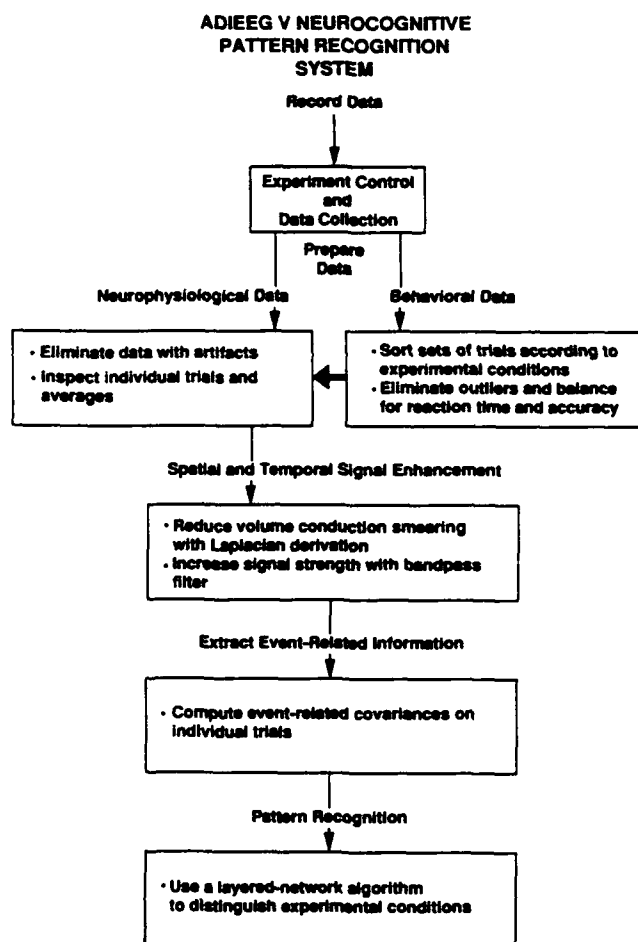


FIGURE 7. ADIEEG-V system for pattern recognition of event-related brain signals. Separate subsystems perform on-line experimental control and data collection, data selection and evaluation, signal processing and pattern recognition. Current capacity is 128 channels.

APPLYING THE TOOLS

Bimanual Visuomotor Task

One of the goals of the bimanual visuomotor experiment was to study prefrontal involvement while subjects prepared to perform a task accurately and used feedback about their accuracy to gauge their responses.¹⁶⁻¹⁸

Subjects and Task

Seven healthy, right-handed, male adults participated in this study. A visual cue, slanted to the right or to the left, prompted the subject to prepare to make a response pressure with the right or left index finger. One sec later, the cue was followed by a visual numeric stimulus (numbers 1-9) indicating that a pressure of 0.1 to 0.9 kg should be made with the index finger of the previously indicated hand. A two-digit number, presented 1 sec after the peak of the response pressure, provided feedback that indicated the subject's exact pressure. On a random 20% of the trials, the stimulus number was slanted in the opposite direction to the cue; subjects were to withhold their responses on these "catch trials." The next trial followed 1 sec after disappearance of the feedback. Each subject performed several hundred trials, with rest breaks as needed.

Recordings

Twenty-six channels of EEG data, as well as vertical and horizontal eye-movements and flexor digitorum muscle activity from both arms, were recorded. All single-trial EEG data were screened for eye-movement, muscle potential, and other artifacts, and contaminated data were discarded.

Analysis and Results

Intervals used for ERC analysis were centered on major event-related potential peaks. ERCs were computed between each of the 120 pairwise combinations of the 16 nonperipheral channels. Intervals were set from 500 msec before the cue to 500 msec after the feedback. We first calculated the mean error (deviation from the required finger pressure) over all trials from the recording session. Individual trials were then classified as accurate (trial error less than mean error) or inaccurate (trial error greater than mean error).

ERC patterns during a 375-msec interval, centered 687 msec post-cue (spanning the late contingent negative variation—CNV), regardless of subsequent accuracy, involved left prefrontal sites, as well as appropriately lateralized central and parietal sites

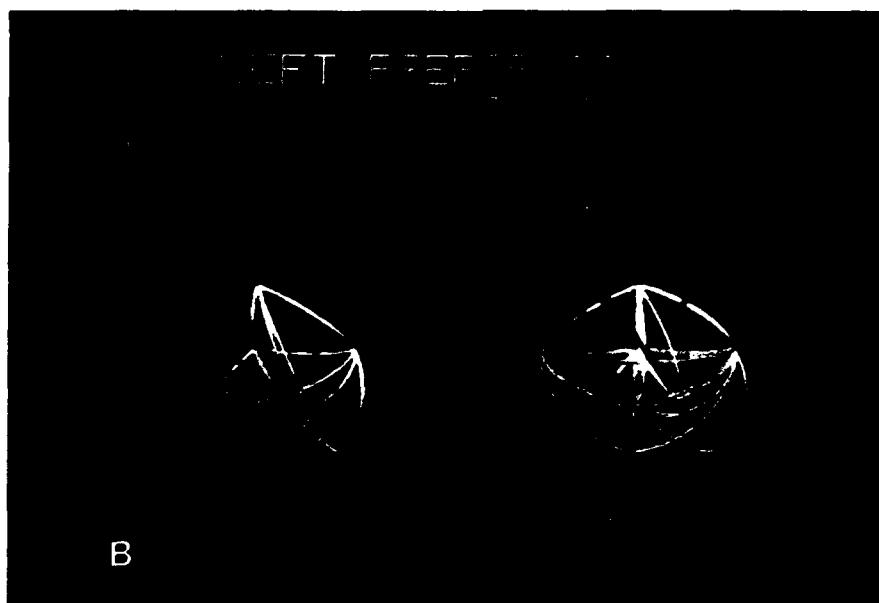
(FIG. 8A and B). Inaccurate performance by the right hand was preceded by a very simple pattern, while inaccurate performance by the left hand was preceded by a complex, spatially diffuse pattern. The relative lack of ERCs preceding inaccurate right-hand performance may simply reflect inattention on those trials, while the strong and complex patterns preceding inaccurate performance with the left hand may reflect effortful, but inappropriate, preparation by the right-handed subjects.

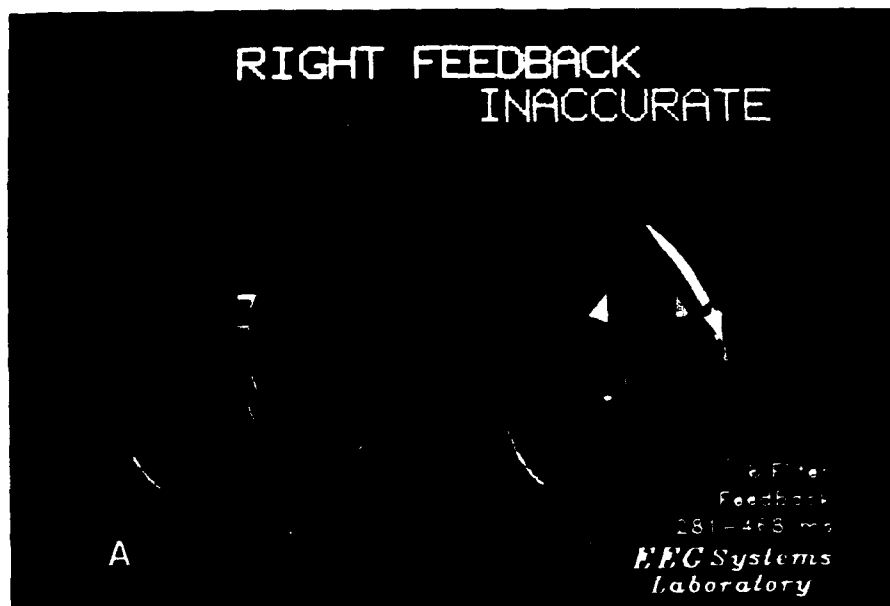
ERC patterns related to feedback about accurate and inaccurate performances were similar immediately after the onset of feedback, but began to differ in an interval, centered at 375 msec, that spanned the P3 (FIG. 9A and B). The ERC patterns for feedback to accurate performance by the two hands were very similar (bootstrap correlation = 0.91 ± 0.01), involving midline antero-central, central, anteroparietal, parietal, and anterooccipital sites; left anteroparietal and antero-central sites; and right parietal, anteroparietal, antero-central, and frontal sites. These accurate patterns involved many long-delay (32-79 msec) ERCs. The waveforms of the frontal and antero-central sites lagged those of more posterior sites. For feedback to inaccurate performance, patterns for both hands were also very similar (bootstrap correlation = 0.90 ± 0.02) and involved most of the same sites as the accurate patterns, with the striking inclusion of the left and midline frontal sites. Again, frontal waveforms lagged those of the more posterior sites with which they covaried. There were even more long-delay ERCs than in the accurate patterns.

Summary

The pre-stimulus ERC patterns seem to characterize a distributed preparatory neural set that is related to the accuracy of subsequent task performance. This network involves distinctive cognitive (frontal), integrative-motor (midline precentral) and lateralized somesthetic-motor (central and parietal) components. The involvement of the left-frontal site is consistent with Teuber's¹⁹ notions of corollary discharge and with other experimental and clinical findings suggesting the synthesis and integration of functional networks in prefrontal cortical areas.²⁰⁻²³ A midline antero-central integrative-motor component is consistent with known involvement of premotor and supplementary motor areas in initiating motor responses. The finding of an appropriately lateralized central and parietal component is consistent with evidence from primates and humans for neuronal firing in motor and somatosensory cortices prior to motor responses.

FIGURE 8. Preparatory event-related covariance (ERC) patterns (colored lines). Measurements are from an interval 500 to 875 msec after the cue for subsequently accurate (A) right-hand and (B) left-hand visuomotor task performance by seven right-handed men. The ERCs are superimposed for illustrative purposes over a horizontal MR scan. The thickness of a covariance line is proportional to its significance (from .05 to .005). A violet line indicates the covariance is positive, while a blue line is negative. ERCs involving left frontal and appropriately contralateral central and parietal electrode sites are prominent in patterns for subsequently accurate performance of both hands. The magnitude and number of preparatory ERCs are greater preceding subsequently inaccurate left-hand performance than those preceding inaccurate right-hand performance by the right-handed subjects. Inaccurate left-hand preparatory ERCs are more widely distributed compared with the left-hand accurate pattern. For the right-hand, fewer and weaker ERCs characterize subsequently inaccurate performance.





Since ERC feedback patterns of accurate or inaccurate performance (involving either hand) were more similar than those between accurate and inaccurate patterns for one hand, it may be inferred that the feedback patterns were related more to performance accuracy than to the hand used. The fact that ERC patterns following disconfirming feedback involved more frontal sites than did patterns following confirming feedback is consistent with the idea that greater resetting of performance-related neural systems is required following disconfirming feedback. Likewise, the front focus of these differences is consistent with the importance of the frontal lobes in the integration of sensory and motor activities.^{20,23}

Effects of Mental Fatigue on Functional Brain Topography

In this study, the effects of mental fatigue on preparation and memory, stimulus recognition and stimulus processing were studied.²⁴

Subjects and Task

Five healthy, right-handed, male subjects performed a task that required that they remember two continuously changing numbers, in the presence of numeric distractors, and produce precise finger pressures. Each trial consisted of a warning symbol, followed by a single-digit visual stimulus to be remembered, followed by the subject's finger-pressure response to the stimulus number presented two trials ago, followed by a two-digit feedback number indicating the accuracy of the response. For example, if the stimulus numbers in five successive trials were 8, 6, 1, 9, 4, the correct response would be a pressure of 0.8 kg when seeing the 1, 0.6 kg for the 9, and 0.1 kg for the 4. To increase the task difficulty, subjects were required to withhold their response on a random 20% of the trials. These "no-response catch trials" were trials in which the current stimulus number was identical to the stimulus two trials ago. Subjects were given ample practice to stabilize accuracy and reaction time.

Subjects performed the task over a 10-14 h period. Sets of trials with equally accurate performance and response movement parameters were selected from three periods: an early period during the first 7 h (Alert), a middle period just prior to any decline in overall performance accuracy (Incipient Performance Impairment), and a late period after performance had significantly degraded.

FIGURE 9. Most significant (top 2 SD) feedback ERC patterns elicited when subjects were given information about the accuracy of their finger pressure response by the right hand (A) and left hand (B). ERCs were derived from a 187-msec-wide interval, beginning 281 msec and ending 468 msec post-feedback, on theta-band-filtered, 7-subject-averaged evoked potential waveforms. The color of the covariance line indicates the lag time of maximum covariance between electrodes: yellow, 0-15 msec; green, 16-31 msec; blue, 32-47 msec; red, 48-79 msec; purple, 80+ msec. A major difference between accurate and inaccurate patterns is that the left and midline frontal sites are only involved in the inaccurate patterns. The involvement of these sites may reflect greater processing after inaccurate performance in order to improve subsequent performance.

Recordings

EEGs were recorded with either 33 or 51 channels set in a nylon mesh cap. Vertical and horizontal eye movements were also recorded, as were the responding flexor digitorum muscle potentials, electrocardiogram, and respiration. Three-axis magnetic resonance image scans were made of three of the five subjects.

Analysis and Results

Neuroelectric effects were observed during two fraction-of-a-second intervals when subjects (1) prepared to receive a new stimulus number while holding the two previous stimulus numbers in working memory (CNV interval), and (2) when they withheld their response in the instance where the current stimulus number was the same as the two-back stimulus number (P300 interval). Significant differences were seen between the early Alert period and the middle Incipient Performance Impairment (IPI) period ($p < 0.0001$). While the magnitude of the patterns was reduced during both preparatory and response inhibition intervals, the topographic distribution of the pattern was only affected during preparation (FIG. 10). The preparatory pattern shifted from one strongly focused on midline central and precentral sites to one focused primarily on right-sided precentral and parietal sites. It appeared as though extended task-performance altered the "neural strategy" used to perform the same behavior. Thus, prolonged mental work differentially affected two successive split-second information processing intervals.

The extent to which each subject's patterns corresponded to the group's and the extent to which it was possible to distinguish individual trials from the Alert and IPI periods of the session were determined next using pattern recognition analysis. ERCs common to the group (FIG. 10, left and middle) were considered as possible variables. For the preparatory interval, they consisted of ERCs computed over the 500 msec pre-stimulus epoch of each trial. For separate groups of three and two subjects whose resting EEG characteristics differed, five equations were formed on four-fifths of the trials, and tested on the remaining one-fifth. The average test set accuracy of Alert versus IPI discrimination was then computed and tested for significance by reference to the binomial distribution. Discrimination accuracy was 62% ($p < 0.001$). Individualized equations were generated on the subject with the most usable data, still using the variables from the group pattern. Discrimination accuracy climbed to 81% ($p < 0.0001$).

Summary

Striking changes occurred in the ERC patterns after subjects performed the difficult memory and fine-motor control task for an average of 7-9 h, but before performance deteriorated. Pattern strength was reduced in a fraction-of-a-second-long response preparation interval over midline precentral areas and over the entire left hemisphere. By contrast, pattern strength in a succeeding response-inhibition interval was reduced over all areas. The pattern changed least in an intervening interval associated with visual-stimulus processing. This suggests that, in addition to the well-known global

reduction in neuroelectric signal strength, functional neural networks are selectively affected by sustained mental work in specific fraction-of-a-second task intervals. For practical application, these results demonstrate the possibility of detecting leading indicator neuroelectric patterns which precede degradation of performance due to sustained mental work.

Neurocognitive Analysis of Elementary Language Processes

Preliminary results of a recent experiment demonstrate good spatial and temporal differentiation of basic linguistic functions using 59-channel EEG recordings.

Subjects and Task

Nine right-handed, healthy male subjects performed a language task in which they had to judge whether the second visually presented stimulus of a given condition (S2) formed a match with the first stimulus (S1). There were four, fully randomized conditions in the experiment. In the graphic non-letter condition, the stimuli were characters of Katakana, a Japanese script with which none of the subjects were familiar. Subjects were required to judge whether or not the stimuli were identical. In the phonemic condition, subjects were required to judge if the pronounceable but neologistic word stimuli sounded alike. In the semantic condition, subjects were required to decide if the high frequency, open-class monosyllabic words were opposite or not. Finally, in the grammatical condition, subjects judged if the verb of the S2 formed a meaningful and grammatically correct sentence with the S1 pronoun. Eighty-five percent of the trials were "match" trials and no response was required; subjects responded to the 15% mismatch trials with a button press using the left index finger.

Recordings

EEGs referenced to the midline anterior-parietal (aPz) electrode were recorded from 59 scalp electrodes. The montage was an extended 10-20 system,² and included the frontal sites aF1 and aF2, Fz, F3 to F8, and Fpz; the anterior central aCz, aC1 to aC6; central Cz, C3 and C4; anterior temporal aT5 and aT6; temporal T3 to T8; lower temporal IT1, IT2, IT5, IT6; ventral temporal vT5 and vT6; anterior parietal aP1 to aP6; parietal Pz, P3 to P6; anterior occipital aO1 and aO2; occipital Oz, O1 and O2; ventral occipital vO1 and vO2; and the inion (I) and both mastoids (M1 and M2). Vertical eye movements were recorded bipolarly from an electrode pair placed supra- and suborbitally; horizontal eye movements were recorded bipolarly between electrodes at the outer canthus of each eye. Other bipolar pairs were placed over flexor digitorum muscles of left and right arms to record EMG and at the submentalis to record subvocal movements of the larynx and mouth. The EEG was amplified 8333 times, band-pass filtered from 0.5-50 Hz and recorded at 128 samples per sec.

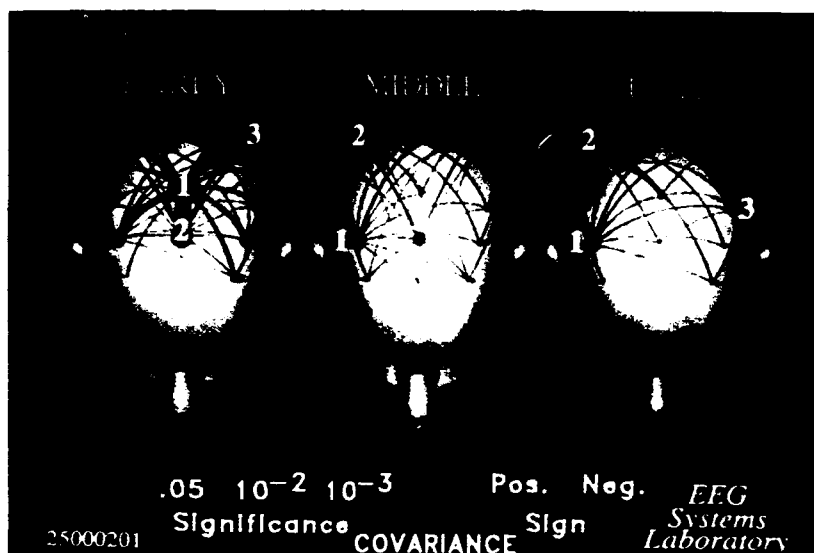


FIGURE 10. Pattern recognition analysis using an artificial, layered neural network that distinguished ERC neuroelectric patterns recorded during baseline (early), incipient performance impairment (middle), and impaired performance (late) periods from five Air Force test pilots performing a difficult visuomotor-memory task over a 14-h period. Baseline data were obtained during the first 7 hours; incipient performance impairment data during hours 7-10 preceding impaired performance; the impaired performance data were obtained during hours 10-14. The ERCs were measured during a 500-msec interval when the subjects were remembering two numbers and preparing for the next stimulus. ERCs greatly declined in magnitude from baseline (early) to incipient performance impairment (middle) to impaired performance (late) epochs. The patterns also changed, with the emphasis shifting from the (1) midline central, (2) midline precentral, and (3) left parietal sites to right hemisphere sites.

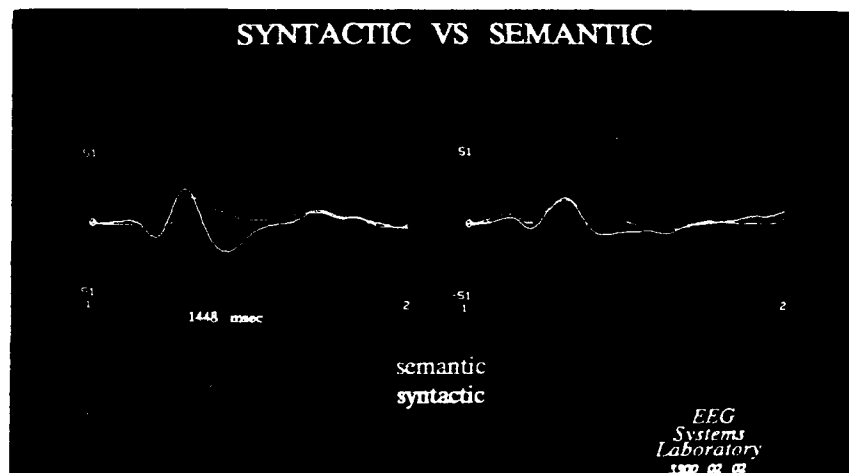


FIGURE 11. LD waveforms evoked by the first of two stimuli (syntactic and semantic) in an experiment designed to study elementary language processes. The waveforms are averaged across nine subjects. The major difference between the grammatic (syntactic) and semantic conditions is lateralized to the left hemisphere, where the grammatic condition has a substantial peak at 442 msec at left frontal and anterior central sites. The x-axis shows 1-sec beginning with the S1. The y-axis corresponds to $\pm 0.153 \mu\text{V}/\text{sq cm}$.

Analysis and Results

Analysis of both ERP and ERC data is ongoing. Among the condition differences observed to date, for example, syntactic and nonsyntactic trials were clearly differentiated by ERP topography. After S1, the grammatic (syntactic) condition alone had a substantial peak at 442 msec at lateral frontal and anterior central sites. N442 was most robust at F3 (Fig. 11), F5, and aC1, where it was significantly larger than in the semantic condition ($p < 0.05$). After S2 (not shown), the grammatic condition was again distinguished from the semantic condition by a positive peak at 279 msec at left frontal and anterior central electrodes. At these sites, the grammatic P279 was larger in amplitude than in the semantic condition ($p < 0.05$). It was not significantly lateralized.

Summary

Stimuli in both the nonsyntactic and syntactic conditions in this experiment were words with similar physical characteristics. The main difference between them post-S1 was that the semantic (nonsyntactic) condition used open-class words (content words such as nouns and adjectives) and the grammatic (syntactic) condition used closed-class words (function words), in this case pronouns. It is possible that the N411 observed for the syntactic condition is related to processing the closed-class words, to the initiation of a "syntactic parser,"²⁵ or to both processes simultaneously. The location of the "syntactic" effect at left frontal sites (F3, F5, and aC3) after both S1 and S2 is consistent with neurophysiological observations of syntactic deficits and difficulties in handling closed-class words in aphasia patients whose lesions involve and extend deep to Broca's area.

CONCLUSIONS

Methodological

Advances in neuroelectric recording and analysis technology during the past two decades have significantly increased the sensitivity and specificity of measuring brain-behavior relationships. Sharper spatial resolution is provided by an increased number of electrodes and by use of the Laplacian derivation. Information about common activity and its temporal relationships is provided by the event-related covariance measure, while neural network pattern recognition analysis provides a powerful method of detecting neurocognitive signals in sets of single-trial data. The signs we have seen of rapidly shifting, functionally interdependent cortical networks are particularly intriguing in light of their consistency with both historical and contemporary, clinical and experimental findings about brain-behavior relationships. In our current research, we hope to further refine and elaborate these methodological and experimental paradigms.

Models of Neural Information Processing in Cognitive Electrophysiology

Because of the stimulus-response design inherent in most experimental designs, many models of cognitive functioning have a passive tone. The brain reacts to a given stimulus, and the stages leading to response are inferred from measures of reaction time, ERP peak latencies, and so on. However, we know from experience, observation, and inference that cognitive processes are highly interactive. Our environment is, in a sense, altered by our perception of it, because perception itself is a synthesis of sensation, current brain state, and past cognitive experience. This synthesis involves a continuously updated, dynamic internal representation of what we imagine our selves and

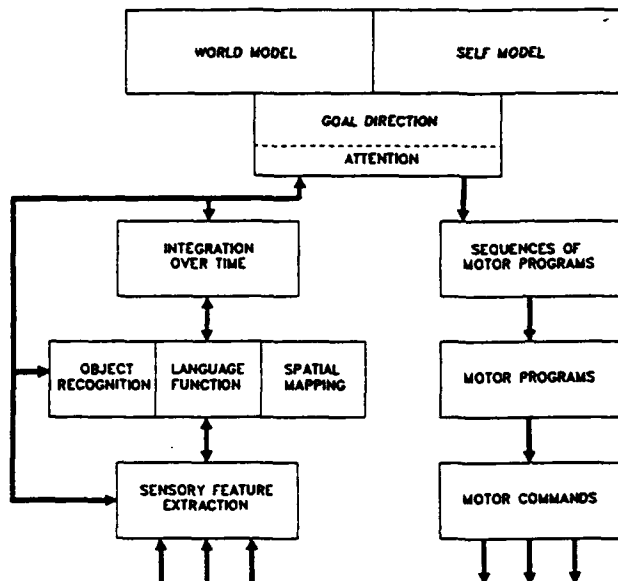


FIGURE 12. Sketch of parallel, sequential, hierarchically organized information processing in functional networks of the human neocortex. The previous moment's internal model influences the current moment's goal direction and attention, which in turn influences other stages of processing.

environment to be like at any given moment. Moreover, we use our effector and sensory systems to probe actively the environment for information relevant to maintaining and updating the self/world model (FIG. 12). Each perception, each action is incorporated into the internal model, and new perceptions and actions are in turn influenced through the model's role in directing attentional and conceptual processes. It is challenging, but not impossible, to design experimental situations which emphasize this dynamic and interactive nature of cognition. Two areas that have been of particular interest to us are preparatory processes, which precede the stimulus and are directed by the internal model, and feedback, which governs the updating of the model after behaviors. Although it is likely that the frontal cortex plays a pivotal role in both processes, it

would be simplistic to consider the frontal lobes as a mere executor. Rather, it is likely that the entire brain is involved in a constellation of rapidly changing, functional networks that provide the delicate balance between stimulus-locked behavior and purely imaginary ideation. The pre-stimulus and the feedback-associated "processing networks" observed in our studies may be signs of such interrelated activity. With even further advances in brain imaging in neuropsychophysiology in the 1990s, we can hope to achieve increasingly detailed and direct measurements of the organization and interrelationships of sensory and higher cognitive behaviors in health and in disease.

ACKNOWLEDGMENTS

The authors gratefully acknowledge the efforts of their scientific collaborators Drs. S. Bressler, P. Brickett, B. Cutillo, R. Fowler-White, D. Greer, J. Le, N. Morgan, and B. Reutter for their contributions to the original research presented here.

REFERENCES

1. JASPER, H. H. 1958. The ten-twenty electrode system of the International Federation of Societies for Electroencephalography. *EEG Clin. Neurophysiol.* 10: 371.
2. GEVINS, A. S. 1988. Recent advances in neurocognitive pattern analysis. *In* Dynamics of Sensory and Cognitive Processing of the Brain. E. Basar, Ed.: 88-102. Springer-Verlag, Heidelberg.
3. HUORTH, B. 1975. An on-line transformation of EEG scalp potentials into orthogonal source derivations. *Electroenceph. Clin. Neurophysiol.* 39: 526-530.
4. HUORTH, B. 1980. Source derivation simplifies topographical EEG interpretation. *Am. J. EEG Technol.* 20: 121-132.
5. DOYLE, J. C. & A. S. GEVINS. 1986. Spatial filters for event-related brain potentials. EEG Laboratory, Technical Report TR86-001.
6. BARLOW, J. S. 1986. Artifact processing (rejection and minimization) in EEG data processing. *In* Handbook of Electroencephalography and Clinical Neurophysiology, Vol. 2. F. H. Lopes da Silva, W. Storm van Leeuwen, A. Remond, Eds.: 15-65. Elsevier, Amsterdam.
7. GEVINS, A. S., G. M. ZEITLIN, J. C. DOYLE, C. D. YINGLING, R. E. SCHAFER, E. CALLAWAY & C. L. YEAGER. 1979. Electroencephalogram correlates of higher cortical functions. *Science* 203: 665-668.
8. GEVINS, A. S., G. M. ZEITLIN, C. D. YINGLING, J. C. DOYLE, M. F. DEDON, R. E. SCHAFER, J. T. ROUMASSET & C. L. YEAGER. 1979. EEG patterns during "cognitive" tasks. I. Methodology and analysis of complex behaviors. *Electroencephalogr. Clin. Neurophysiol.* 47: 693-703.
9. GEVINS, A. S., J. C. DOYLE, B. A. CUTILLO, R. F. SCHAFER, R. L. TANNEHILL, J. H. GHANNAM, V. A. GILCREASE & C. L. YEAGER. 1981. Electrical potentials in human brain during cognition: New method reveals dynamic patterns of correlation. *Science* 213: 918-922.
10. GEVINS, A. S. & S. L. BRESSLER. 1988. Functional topography of the human brain. *In* Functional Brain Imaging. G. Pfurtscheller, Ed.: 99-116. Hans Huber Publishers, Bern.
11. GEVINS, A. S., N. H. MORGAN, S. L. BRESSLER, J. C. DOYLE & B. A. CUTILLO. 1986. Improved event-related potential estimation using statistical pattern classification. *EEG Clin. Neurophysiol.* 6: 177-186.

12. EFRON, B. 1982. The Jackknife, the Bootstrap, and Other Resampling Plans. Society for Industrial and Applied Mathematics. Philadelphia, PA.
13. GEVINS, A. S. 1987. Statistical pattern recognition. *In Handbook of Electroencephalography and Clinical Neurophysiology*. Vol 1. A. Gevins & A. Remond, Eds. Elsevier. Amsterdam.
14. GEVINS, A. S. & N. H. MORGAN. 1988. Applications of neural network (NN) signal processing in brain research. *IEEE ASSP Trans.*, 36(7): 1152-1161.
15. GEVINS, A. S. 1980. Pattern recognition of brain electrical potentials. *IEEE Trans. Patt. Anal. Mach. Intell.* 2(5): 383-404.
16. GEVINS, A. S., N. H. MORGAN, S. L. BRESSLER, B. A. CUTILLO, R. M. WHITE, J. ILLES, D. S. GREER, J. C. DOYLE & G. M. ZEITLIN. 1987. Human neuroelectric patterns predict performance accuracy. *Science* 235: 580-585.
17. GEVINS, A. S., B. A. CUTILLO, S. L. BRESSLER, N. H. MORGAN, R. M. WHITE, J. ILLES & D. S. GREER. 1989. Event-related covariances during a bimanual visuomotor task. Part I: Methods & analysis of stimulus- and response-locked data. *EEG Clin. Neurophysiol.* 74(1): 58-75.
18. GEVINS, A. S., B. A. CUTILLO, S. L. BRESSLER, N. H. MORGAN, R. M. WHITE, J. ILLES & D. S. GREER. 1989. Event-related covariances during a bimanual visuomotor task. Part II: Preparation and feedback. *EEG Clin. Neurophysiol.* 74(2): 147-160.
19. TEUBER, H. L. 1964. *In The Frontal Granular Cortex and Behavior*. J. Warren & K. Akert, Eds. McGraw-Hill. New York, NY.
20. FUSTER, J. M. 1989. *The Prefrontal Cortex: Anatomy, Physiology, and Neuropsychology of the Frontal Lobe*. Raven Press. New York, NY.
21. GOLDMAN-RAKIC, P. S. 1988. Topography of cognition: Parallel distributed networks in primate association cortex. *Annu. Rev. Neurosci.* 11: 137-156.
22. GOLDMAN-RAKIC, P. S. 1988. Changing concepts of cortical connectivity: Parallel distributed cortical networks. *In Neurobiology of Neocortex*. P. Rakic and W. Singer, Eds.: 177-202. John Wiley. New York, NY.
23. STUSS, D. & D. F. BENSON. 1986. *The Frontal Lobes*. Raven Press. New York, NY.
24. GEVINS, A. S., S. L. BRESSLER, B. A. CUTILLO, J. ILLES & R. M. FOWLER-WHITE. 1989. Effects of prolonged mental work on functional brain topography. *EEG Clin. Neurophysiol.* 76: 339-350.
25. GARRETT, M. F. 1982. Production of speech: Observations from normal and pathological use. *In Normality and Pathology in Cognitive Functions*. A. W. Ellis, Ed., Vol. 9. Academic Press. New York, NY.